Materials Science in Semiconductor Processing 187 (2025) 109121

Contents lists available at ScienceDirect

Materials Science in Semiconductor Processing

journal homepage: www.elsevier.com/locate/mssp

Effect of 5 MeV proton irradiation on electrical and trap characteristics of β-Ga_2O_3 power diode

Haolan Qu [a,b,c], Wei Huang [d], Yu Zhang [a], Jin Sui [a], Ge Yang [a], Jiaxiang Chen [a], David Wei Zhang [d], Yuangang Wang [e], Yuanjie Lv [e], Zhihong Feng [e], Xinbo Zou [a,f,*]

[a] School of Information Science and Technology, ShanghaiTech University, 201210, Shanghai, People's Republic of China
[b] Shanghai Institute of Microsystem and Information Technology, Chinese Academy of Sciences, 200050, Shanghai, People's Republic of China
[c] School of Microelectronics, University of Chinese Academy of Sciences, 100049, Beijing, People's Republic of China
[d] School of Microelectronics, Fudan University, 200433, Shanghai, People's Republic of China
[e] The National Key Laboratory of Application Specific Integrated Circuit (ASIC), Hebei Semiconductor Research Institute, 050051, Shijiazhuang, Hebei, People's Republic of China
[f] Shanghai Engineering Research Center of Energy Efficient and Custom AI IC, 200031, Shanghai, People's Republic of China

ARTICLE INFO

Keywords:
Proton irradiation
β-Ga_2O_3
Static characteristics
Trap characteristics
Dynamic characteristics

ABSTRACT

In this study, impact of 5 MeV proton irradiation with radiation fluence of 10^{13} cm^{-2} on β-Ga_2O_3 power diode is investigated by a β-Ga_2O_3 Schottky barrier diode (SBD). Via temperature-dependent measurements, carrier removal rate R_C is determined to be 7.26 × 10^2 cm^{-1} at 300 K. Meanwhile, the threshold voltage (V_{on}) and ideality factor (n) almost remain stable after proton irradiation. A close-to-unity n was observed for a wide temperature range indicating near-ideal Schottky characteristics. Dynamic degradation was observed at 300K, but was greatly suppressed at a low temperature of 100K. Meanwhile, two more bulk traps are discovered in proton irradiated β-Ga_2O_3 SBD by deep-level transient spectroscopy (DLTS). The larger corrected trap concentration (N_{Ta}) in proton irradiated β-Ga_2O_3 SBD was regarded as the reason behind slightly worsened dynamic on-resistance instability at 300 K. Furthermore, lower low frequency noise is revealed for proton irradiated device at room temperature and cryogenic temperature. The study demonstrates the competitive irradiation hardness of β-Ga_2O_3 power diodes and paves a solid path for the deployment of β-Ga_2O_3 in space.

1. Introduction

β-Ga_2O_3 has gained significant recognition as an ultra-wide bandgap (4.9 eV) semiconductor material for developing next generation power electronics owing to its large breakdown electric field of 8 MV/cm and high-temperature stability [1–3]. Continuous progress in the fabrication technologies and epitaxial layers have led to implementation of high performance β-Ga_2O_3 power devices. An enhancement mode β-Ga_2O_3 U-shaped gate trench metal-oxide-semiconductor field-effect transistor has been successfully demonstrated with a positive threshold voltage ($\boldsymbol{V_{on}}$ = 4.2 V), a high current density (I_{DS} = 702.3 A/cm^2), a low on-resistance (R_{on} = 10.4 mΩcm^2), and a large breakdown voltage (V_{br} = 455 V) [4].

Meanwhile, β-Ga_2O_3 is anticipated to hold high radiation tolerance due to its ultra-wide bandgap [5]. In previous reports, β-Ga_2O_3 is concluded to possess radiation resistance comparable to or even superior to GaN or SiC, surpassing GaAs and Si [6,7], demonstrating huge potential of β-Ga_2O_3 for space applications [8,9]. The influence of various types of radiation on β-Ga_2O_3 have been documented, including neutron irradiation [10–14], proton irradiation [15–18], electron irradiation [19,20], ion irradiation [21,22], and α-particle irradiation [17]. Degradation of electrical characteristics including $\boldsymbol{V_{on}}$, reverse current, Schottky barrier height (Φ_B), and ideality factor (n) of electron irradiated β-Ga_2O_3 were observed [20]. Additionally one trap was identified in Ge-doped β-Ga_2O_3 after neutron irradiation [10]. A trap level with ionization energy around 0.75 eV also emerged in β-Ga_2O_3 after proton irradiation, by provoking the generation of intrinsic defect [18].

Despite that some studies on proton irradiated β-Ga_2O_3 have been reported, there are still some important issues, waiting to be addressed, such as study of wide temperature feasibility, dynamic characteristics, etc. The impact of proton irradiation on characteristics of β-Ga_2O_3 still need to be further investigated.

* Corresponding author. School of Information Science and Technology, ShanghaiTech University, 201210, Shanghai, People's Republic of China.
E-mail address: zouxb@shanghaitech.edu.cn (X. Zou).

https://doi.org/10.1016/j.mssp.2024.109121
Received 4 August 2024; Received in revised form 30 September 2024; Accepted 12 November 2024
Available online 19 November 2024

J. F. McGlone et al. studied the impact of 1.8 MeV proton irradiation on the electrical properties of β-Ga_2O_3 SBD at room temperature [23]. However, the research of electrical performance covering a wide temperature range is still missing. The comprehension of electrical characteristics covering a wide temperature range is important for the low-temperature application of β-Ga_2O_3-based devices.

The dynamic characteristics are critical for the realistic application of β-Ga_2O_3-based devices. The degradation of pristine β-Ga_2O_3 were investigated with different forward and reverse stresses [24–26]. Nevertheless, the dynamic characteristics of proton irradiated β-Ga_2O_3 remains unknown. The causation of degradation after proton irradiation is unavailable, hindering a complete evaluation of β-Ga_2O_3 for harsh environments.

In this paper, the effect of 5 MeV proton irradiation with irradiance of 10^{13} cm^{-2} on β-Ga_2O_3 by a large-size (2×2 mm^2) β-Ga_2O_3 Schottky barrier diode (SBD). Temperature-dependent capacitance-voltage (*C-V*) and current-density-voltage (*J-V*) characteristics β-Ga_2O_3 SBD are reported from 50 K to 350 K. Via on-the-fly measurement, the dynamic performance induced by the bulk traps is elucidated at 100 K and 300 K. Deep-level transient spectroscopy (DLTS) is employed to investigate the impact of proton irradiation on the deep level traps in β-Ga_2O_3 epilayer, and two new traps exists after proton irradiation. The low frequency noise is also applied to discuss the effect of proton irradiation.

2. Device fabrication

Fig. 1 shows the schematic of the proton irradiated β-Ga_2O_3 SBD utilized in this study. The pristine β-Ga_2O_3 SBD contain a 7 μm-thick β-Ga_2O_3 homogeneous epilayer and a β-Ga_2O_3 substrate. Ti/Au was deposited on the backside of the substrate to establish the ohmic contact. To achieve square Schottky contact (2×2 mm^2), Ni/Au was fabricated on the homogeneous epilayer. Proton irradiation was conducted by a 5 MeV proton beam with a radiation fluence (Φ) of 10^{13} cm^{-2} to adapt the environment of Earth's radiation belts in low-Earth orbit [27]. Meanwhile, the projected range of 5 MeV proton irradiation is sufficient to influence the whole homogeneous epilayer [8].

3. Result and discussion

3.1. Static characteristics

Fig. 2 (a) illustrates the *C-V* characteristics of β-Ga_2O_3 SBD before and after proton irradiation with a measurement frequency (*f*) of 1 MHz. It can be observed that the capacitance of irradiated β-Ga_2O_3 SBD is smaller than the pristine one. The capacitance-temperature (*C-T*) curves at −1 V are depicted in Fig. 2 (b). At the bias of −1 V, the *C* of irradiated β-Ga_2O_3 SBD slightly increases from 15.79 nF/cm^2 to 17.43 nF/cm^2 when temperature rises from 50 K to 350 K, and the correlation with temperature of *C* exhibits similarities before and after proton irradiation. Fig. 2 (c) and (d) show the N_s, V_{bi}, and Φ_B, which can be extracted from the following equations [28]:

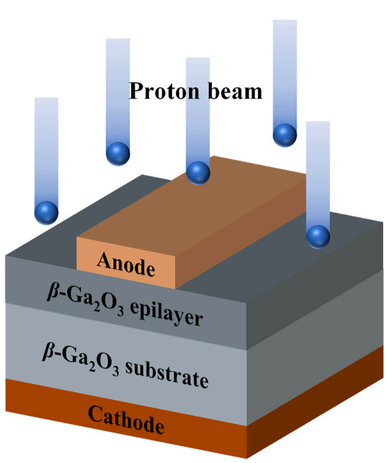

Fig. 1. The schematic of the proton irradiated β-Ga_2O_3 SBD.

$$\frac{1}{C^2} = \frac{2}{\varepsilon_r \varepsilon_0 q A^2 N_S}\left(V + V_{bi} - \frac{kT}{q}\right) \tag{1}$$

$$q\Phi_B = qV_{bi} + E_C - E_F = qV_{bi} - kTln\left(\frac{N_S}{N_C}\right) \tag{2}$$

where ε_r and ε_0 represent relative and vacuum permittivity, respectively, q represents the elementary charge, A represents the anode area, k represents the Boltzmann constant, E_C represents the conduction band minimum, E_F represents the Femi level, and N_C represents the effective density of states in the conduction band. As shown in Fig. 2 (c), the N_s of irradiated β-Ga_2O_3 SBD is extracted to be 6.63×10^{15} cm^{-3} at 300 K. From 50 K to 350 K, the N_s remains almost stable, indicating the negligible carrier freezing-out issue for β-Ga_2O_3 SBD [29]. Meanwhile, the N_s of irradiated β-Ga_2O_3 SBD is much smaller than the pristine one due to the carrier removal effect. The carrier removal effects can be explained by the Fermi-level pinning far from the conduction band minimum due to lattice defect [6], indicating the increased traps. The carrier removal rate R_C could be determined by the equation [30]:

$$R_C = \frac{\Delta N_S}{\Phi} \tag{3}$$

where $\triangle N_S$ is the variation of the carrier concentration before and after proton irradiation. The R_C is derived to be 7.26×10^2 cm^{-1} at 300 K, exhibiting a comparable value with other β-Ga_2O_3 devices after proton irradiation, demonstrating a competitive irradiation hardness of β-Ga_2O_3 SBD [6,31]. Moreover, the R_C reflects weak temperature dependence, demonstrating the steady irradiation hardness for all temperatures due to the stable N_S for both samples. As exhibited in Fig. 2 (d), the $q\Phi_B$ of irradiated β-Ga_2O_3 SBD is extracted to be 0.81 eV at 350 K and 0.85 eV at 50 K. Meanwhile, the $q\Phi_B$ of irradiated β-Ga_2O_3 SBD (0.81 eV at 300 K) is larger than the pristine one (0.65 eV at 300 K). The increase of $q\Phi_B$ is caused by the rapid decrease of N_s after proton irradiation due to image force and tunneling effect [32].

Fig. 3 (a) plots the forward current conduction characteristics of both samples. The V_{on} of irradiated β-Ga_2O_3 SBD, which is defined at 1 A/cm^2 is extracted to be 0.77 V at 300 K. The detailed results of V_{on} are displayed as red squares in Fig. 3 (b). As shown in Fig. 3 (b), the V_{on} decreases from 1.20 V at 50 K to 0.71 V at 350 K. Meanwhile, the temperature-dependent V_{on} before and after proton irradiation is close to each other. To further study the forward conduction mechanism, the thermionic emission model is used to describe the forward *J-V* curves [33]:

$$J = J_S\left(e^{\frac{qV}{nkT}} - 1\right) \tag{4}$$

From the linear fitting, n and J_s can be extracted from the slope and intercept. As shown in Fig. 3 (b), the n of irradiated β-Ga_2O_3 SBD decreases from 1.58 to 1.00 as temperature rises from 50 K to 350 K, which is the result of temperature-enhanced current conduction occurring at the interface of metal and semiconductor [34] and the inhomogeneity caused by the physical defects between metal and semiconductor [35]. Meanwhile, the close-to-unity n demonstrates the near-ideal Schottky characteristics, indicating the huge potential of β-Ga_2O_3 SBD for applications across a wide temperature range. At the same time, the close-to-unity n remains almost unchanged before (1.02 at 300 K) and after (1.05 at 300 K) proton irradiation. The negligible variation of V_{on} and n indicate that proton irradiation has less influence on the forward conduction of β-Ga_2O_3 SBD.

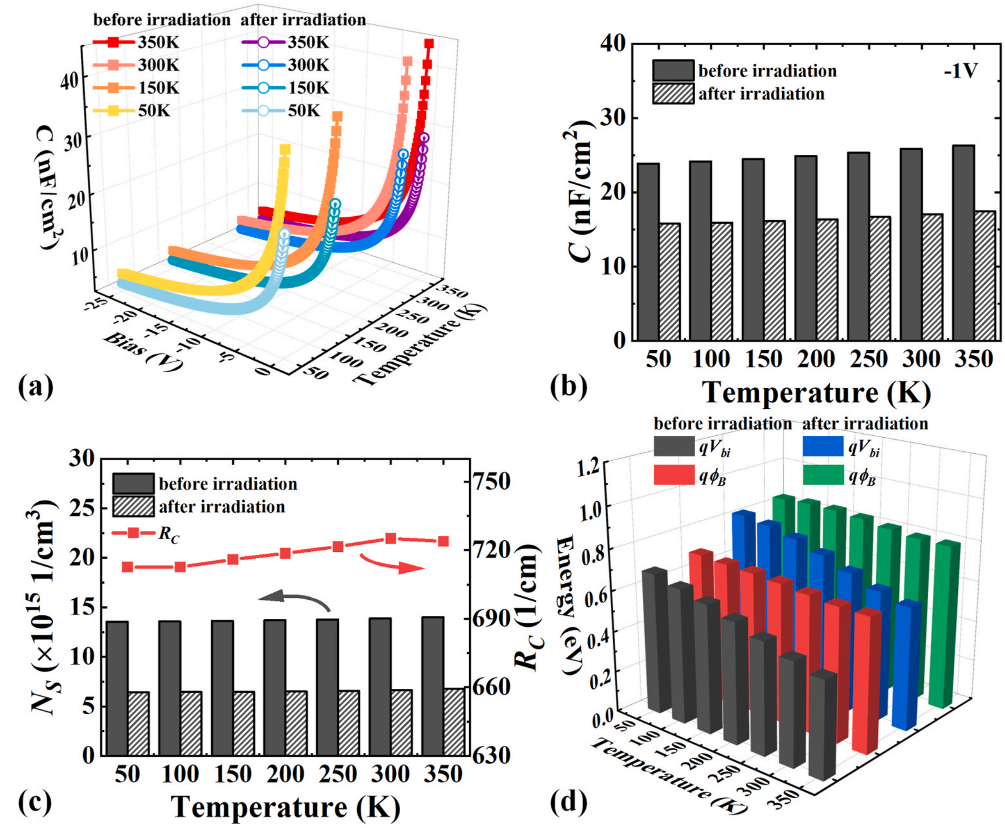

Fig. 2. (a) Temperature-dependent *C-V* curves before and after proton irradiation. (b) Capacitance at −1 V from 50 K to 350 K. (c) Net donor concentration (N_s) and carrier removal rate (R_C). (d) Temperature-dependent built-in voltage (V_{bi}) and Φ_B.

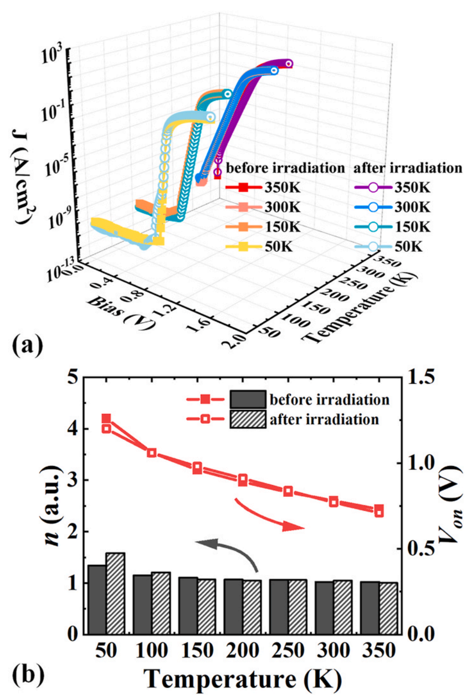

Fig. 3. (a) Temperature-dependent forward *J-V* curves before and after proton irradiation in the logarithmic scale. (b) V_{on} and n.

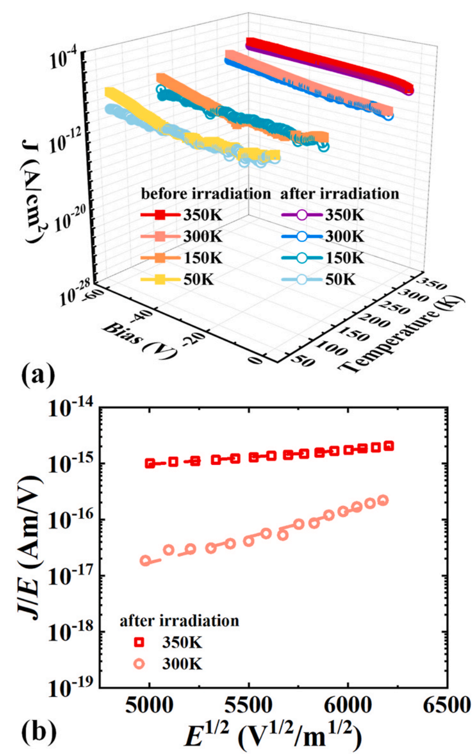

Fig. 4. (a) Temperature-dependent reverse *J-V* curves before and after proton irradiation. (b) ln(J/E) versus $E^{1/2}$ at 300 K and 350 K after proton irradiation.

Fig. 4 (a) exhibits the reverse *J-V* characteristics of both samples. The *J* of irradiated β-Ga_2O_3 SBD climbs from 2.65×10^{-10} A/cm^2 to 7.82×10^{-8} A/cm^2 with the increased temperature from 50 K to 350 K at the bias of –60 V, inferring an excellent off-state performance at cryogenic temperature. Furthermore, the *J* values of pristine and irradiated β-Ga_2O_3 SBD at -60 V bias are extracted to be 4.00×10^{-8} A/cm^2 and 8.40×10^{-9} A/cm^2 at 300 K, respectively. The *J* shows a smaller value after proton irradiation, indicating an improved off-state performance. The leakage current of β-Ga_2O_3 SBD around room temperature can be modelled by Poole-Frenkel emission (PFE) model [36]:

$$J = C'Ee^{-\frac{q}{kT}\left(\Phi_T - \sqrt{\frac{qE}{\pi\varepsilon_r\varepsilon_0}}\right)} \tag{5}$$

where C' represents a constant, E represents the electric field and Φ_T represents the effective barrier height of electron emission from trap state. As shown in Fig. 4 (b), the ln(J/E) versus $E^{1/2}$ exhibits an outstanding linearity for proton irradiation β-Ga_2O_3 SBD, indicating the.

perfect performance of PFE model to describe the leakage characteristics around room temperature.

3.2. Dynamic characteristics

On-the-fly measurement is also performed to investigate the dynamic performance of the β-Ga_2O_3 SBD. Fig. 5 (a) shows the dynamic on-resistance ratio of irradiated β-Ga_2O_3 SBD, which is defined as $R_{on,d}/R_{on,s}$, where $R_{on,d}$ and $R_{on,s}$ represent the on-resistance at the on-the-fly measurement and fresh state, respectively. The brown plane represents the situation that the ratio is 1. When the sample is exposed to different reverse stressing voltage (U_s), the depletion region becomes wider, and bulk traps in the depletion region are unfilled due to the emission of bulk traps, leading to the rising dynamic on-resistance ratio [37]. When the stressing time is 500 s, the ratio with U_s of -50 V, -70 V, and -100 V reach 1.08, 1.10, and 1.11, respectively. When U_s enlarges, the depletion region widens, leading to the rising number of empty bulk traps, resulting in the variation of the ratio. Meanwhile, during the recovery stage, the ratio approaches unity with the increasing recovery time. As exhibited in Fig. 5 (b), different from the increase at 300 K, the dynamic on-resistance ratio of irradiated β-Ga_2O_3 SBD stabilized around unity during stressing stage at 100 K. Although the dynamic on-resistance ratio with U_s of –50 V and–70 V at 100 K is smaller than unity, the value closed to unity is acceptable. The stable dynamic on-resistance ratio indicates the outstanding dynamic performance at 100 K.

Fig. 5 (c) and (d) compare the dynamic on-resistance ratio before and after proton irradiation. As shown in Fig. 5 (c), with the fixed U_s, the variation of ratio of irradiated β-Ga_2O_3 SBD is larger than the pristine one, which is caused by the larger number of bulk traps after proton irradiation. As plotted in Fig. 5 (d), with the fixed U_s, the dynamic on-resistance ratio of irradiated β-Ga_2O_3 SBD needs more time to approach unity than the pristine one.

3.3. Trap characteristics

In order to compare the traps in pristine and irradiated β-Ga_2O_3 SBD, DLTS are employed from 40 K to 350 K due to the upper limitation of the temperature tolerance of equipment. The results of temperature-scanning DLTS are presented in Fig. 6 (a) with a reverse bias $U_R = -20$ V, a filling pulse $U_P = -0.5$ V, a filling pulse width $t_P = 0.1$ s, and a measurement period $T_W = 4$ s. Three majority carrier (electron) traps (E1, E2 and E3) are observed after irradiation while only one majority carrier (electron) trap (E2) is found before irradiation. The Arrhenius

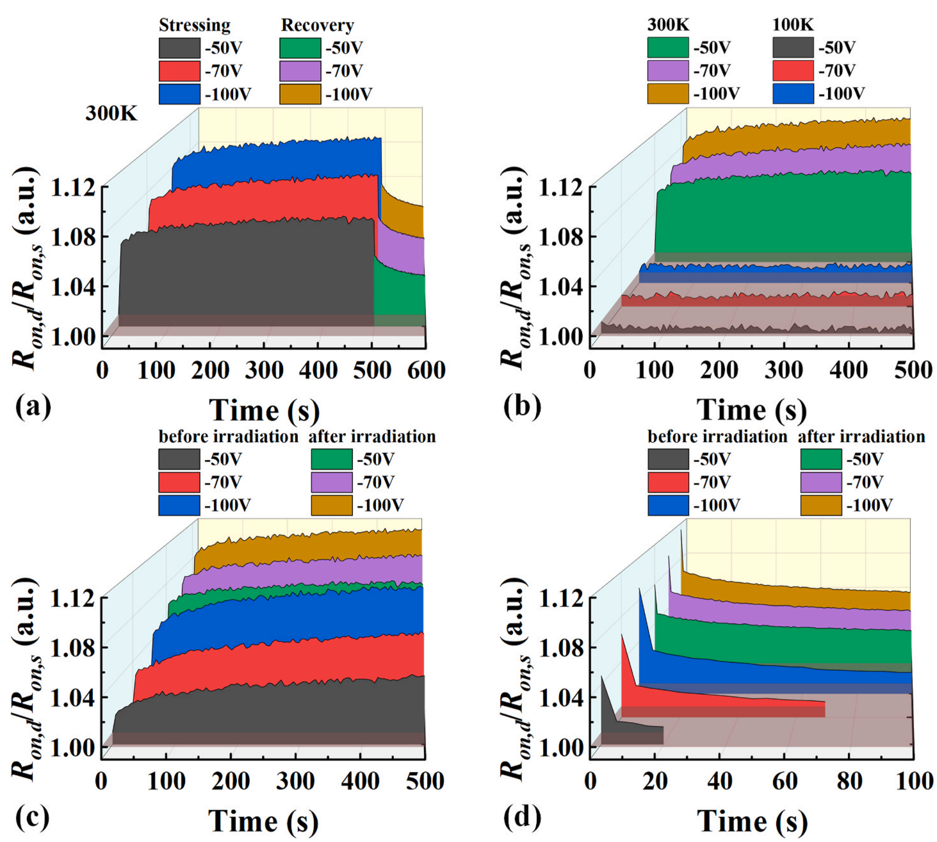

Fig. 5. (a) Dynamic on-resistance ratio of irradiated β-Ga_2O_3 SBD with measurement voltage (U_m) of 0.67 V at 300 K during the stressing process and recovery process. (b) Dynamic on-resistance ratio of irradiated β-Ga_2O_3 SBD at 100 K and 300 K during the stressing process. Dynamic on-resistance ratio with U_m of 0.67 V at 300 K during (c) the stressing process and (d) the recovery process before and after proton irradiation.

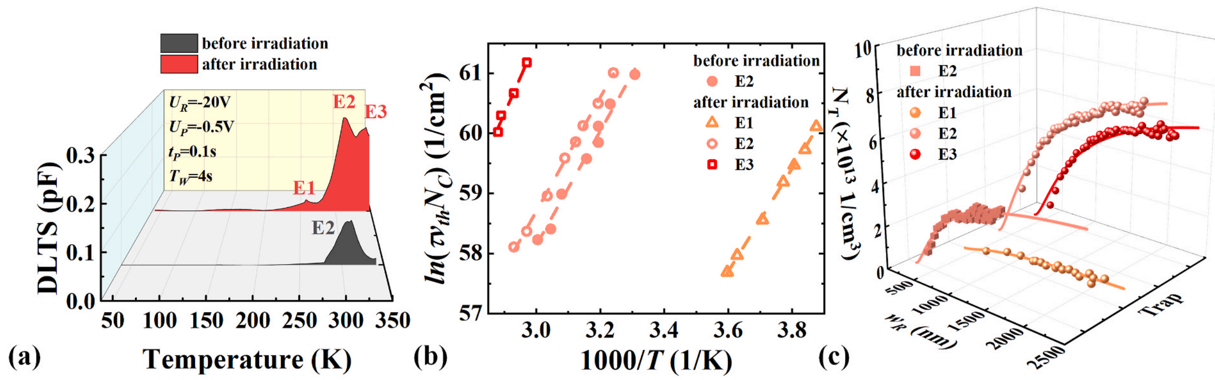

Fig. 6. (a) Temperature-scanning DLTS before and after proton irradiation. (b) Arrhenius plot of the traps before and after proton irradiation. (c) Trap concentration (N_T) versus depletion region width with reverse bias (w_R).

Table 1
The summary of the traps before and after proton irradiation.

Trap	E_{emi} (eV)	σ_n (cm^2)	N_{Ta} (cm^{-3})
E1 (after irradiation)	0.74	2.26×10^{-12}	1.21×10^{13}
E2 (before irradiation)	0.82	1.32×10^{-13}	5.32×10^{13}
E2 (after irradiation)	0.81	6.42×10^{-14}	1.05×10^{14}
E3 (after irradiation)	1.04	9.18×10^{-12}	8.56×10^{13}

plot of traps is shown in Fig. 6 (b), the activation energy for emission (E_{emi}) and the capture cross section (σ_n) are summarized in Table 1. Fig. 6 (c) displays N_T of traps versus w_R. The corrected trap concentration (N_{Ta}) can be calculated by considering lambda effect [38]:

$$N_T = N_{Ta}\left(1 - \frac{\lambda}{w_R}\right)^2 \tag{6}$$

where λ donates non-emission region width. The fitting results are also summarized in Table 1.

As shown in Table 1, more traps are observed in irradiated β-Ga_2O_3 SBD, which is caused by the lattice damage resulting from the high energy protons [8]. The complex structure of β-Ga_2O_3 also provides the possibility to form more traps after proton irradiation. The increased number of traps leads to the carrier removal effect, while the rise of N_{Ta} is smaller than the decrease of N_S. The possible reason might be that there are more traps located in the middle of bandgap not being detected. The increase in the number of traps also matches well with the dramatic decrease of N_S after proton irradiation. Meanwhile, the high N_{Ta} after proton irradiation leads to an increasing number of empty traps, resulting in the larger variation, as shown in Fig. 5 (c). Otherwise, three bulk traps are observed above 200 K, explaining the outstanding dynamic performance at 100 K. E1 was found only after proton irradiation with a relatively small N_{Ta}. According to other researches, E1 is considered to be generated by proton irradiation, which is related to V_{Ga} or Ga_O [15,18]. Meanwhile, E1 is found to have larger σ_n than E2 [15, 18], which is consistent with our results. Around 305 K, E2 is found in both samples in this work, while it has a smaller σ_n and a larger N_{Ta} in irradiated β-Ga_2O_3 SBD. E2 is also observed in other samples before and

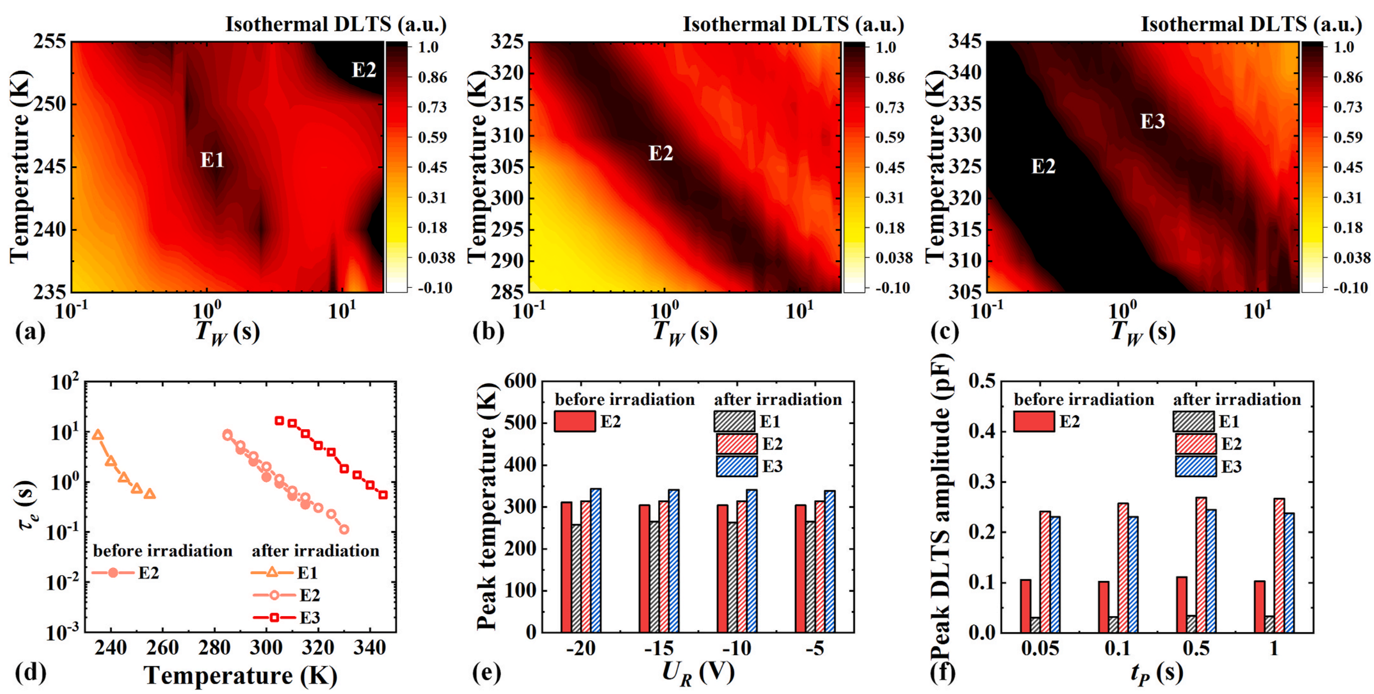

Fig. 7. Contour map of isothermal DLTS of traps in irradiated SBD for (a) E1, (b) E2 and (c) E3. (d) Emission time constant (τ_e) of traps before and after proton irradiation. (e) Peak temperature of traps at different U_R before and after proton irradiation. (f) Peak DLTS amplitude of traps with different t_P before and after proton irradiation.

after proton irradiation [16], demonstrating that the origin of E2 is not related to the proton irradiation. Due to the absence of Fe in our devices, E2 is considered to be associated with complexes involving native defects in β-Ga_2O_3 [16,39]. E3 has been observed both in pristine and irradiated β-Ga_2O_3 SBD in previous works [16,17], while it could only be found in pristine β-Ga_2O_3 SBD in our work. The possible reason for the absence of E3 in pristine β-Ga_2O_3 SBD may be that E3 is located at the temperature above 350 K. An increase is recorded around 340 K before irradiation in Fig. 6(a), which may be the rising edge of E3. According to the energy level, E3 may be oxygen vacancy V_O donors which is responsible for the lifetime degradation of irradiated β-Ga_2O_3 [17].

Fig. 7(a) and (b) and (c) display the contour map of isothermal DLTS of three traps in the irradiated SBD to investigate the temperature-dependent emission process of traps. The black region in each figure represents the positive peak of traps. The τ_e of traps extracted from the positive peak of isothermal DLTS is shown in Fig. 7 (d). As exhibited in Fig. 7 (d), the τ_e of traps before and after proton irradiation decrease with increasing temperature. For instance, from 305 K to 345 K, the τ_e of E3 decreases from 16.56 s to 0.55 s. The increase in τ_e indicates that the emission process of traps can be accelerated by higher temperature. From 290 K to 315 K, the τ_e of E2 after proton irradiation is longer than before irradiation, demonstrating that proton irradiation decelerates the emission process within this temperature range.

Fig. 7 (e) exhibits the peak temperature of traps at different conditions. The peak temperature is barely shifted for all traps at different U_R, supporting the conclusion that all the traps are more likely to be bulk traps instead of interface traps, and their emission processes are independent of electric field [40].

Fig. 7 (f) depicts the peak DLTS amplitude of traps from t_P of 0.05 s to 1 s. The peak DLTS amplitudes of E1 and E3 remain unchanged, thereby concluding that most of the traps are filled within 0.05 s. The peak DLTS amplitude of E2 in irradiated SBD increases with a longer t_P when t_P is shorter than 0.5 s, comparing to the stability in pristine one, indicating that E2 needs more time to be filled after proton irradiation.

3.4. Low frequency noise characteristics

The low frequency noise spectra of both samples are investigated at 100 K and 300 K. Fig. 8 (a) depicts S_I spectra for both samples at different biases at 300 K. For irradiated β-Ga_2O_3 SBD, S_I increases from 2.59×10^{-21} A^2/Hz to 2.48×10^{-19} A^2/Hz with the increasing bias from 0.55 V to 0.75 V with f of 10^5 Hz owing to the higher current. For all biases, the irradiated β-Ga_2O_3 SBD exhibits lower noise level than the pristine one at 300 K, demonstrating better noise performance of irradiated β-Ga_2O_3 SBD at forward bias. The low frequency noise is often influenced by the current of devices and the generation-recombination centers rather than all deep levels. The better low frequency noise performance with increasing N_{Ta} after proton irradiation indicates that E1 and E3 may not produce the generation-recombination noise. Fig. 8 (b) shows the noise spectra at 0.65 V at 100 K and 300 K. When the temperature climbs from 100 K to 300 K, S_I of irradiated β-Ga_2O_3 SBD increases from 8.88×10^{-29} A^2/Hz to 7.52×10^{-20} A^2/Hz with f of 10^5 Hz due to the rising current. At 100 K, S_I of irradiated β-Ga_2O_3 SBD is about one order of magnitude smaller than the pristine one, and the difference extend to three to four orders of magnitude smaller at 300 K, reflecting that the irradiated β-Ga_2O_3 SBD exhibits outstanding noise performance at all temperatures.

4. Conclusion

In summary, the impact of 5 MeV proton irradiation on β-Ga_2O_3 power diode is investigated. From temperature-dependent *C-V* characteristics, the carrier removal effect exists in the irradiated β-Ga_2O_3 SBD. Meanwhile, temperature-dependent *J-V* characteristics demonstrate that the irradiation has less influence on V_{on} and n. The close-to-unity n indicates the near-ideal Schottky characteristics of β-Ga_2O_3 SBD and the great potential of β-Ga_2O_3 SBD for wide temperature range application. Via on-the-fly measurement, the dynamic on-resistance ratio of irradiated β-Ga_2O_3 SBD induced by the bulk traps is larger than the pristine one at 300 K. Besides E2 in the pristine β-Ga_2O_3 SBD, two more bulk traps called E1 and E3 are observed in irradiated β-Ga_2O_3 SBD. The due to the larger N_{Ta} in irradiated β-Ga_2O_3 SBD leads to the slightly worsened dynamic performance at 300 K. Furthermore, the irradiated β-Ga_2O_3 SBD has outstanding noise performance at both room and cryogenic temperatures.

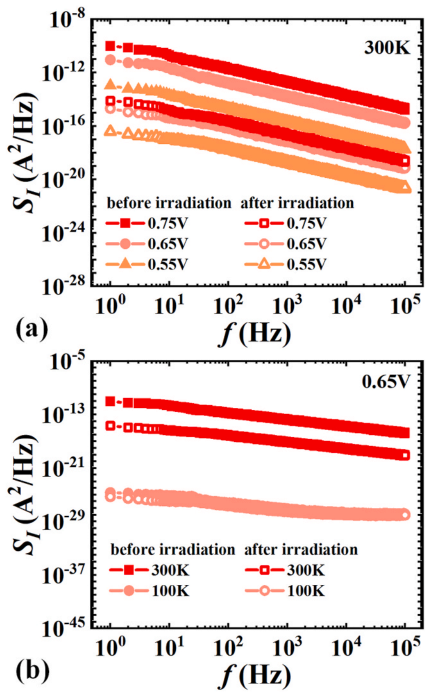

Fig. 8. (a) Noise current density (S_I) spectra at 300 K before and after proton irradiation. (b) S_I spectra at 0.65 V before and after proton irradiation.

CRediT authorship contribution statement

Haolan Qu: Writing – review & editing, Writing – original draft, Visualization, Methodology, Investigation, Formal analysis, Data curation, Conceptualization. **Wei Huang:** Writing – review & editing, Resources, Methodology, Conceptualization. **Yu Zhang:** Writing – review & editing, Methodology. **Jin Sui:** Writing – review & editing, Methodology. **Ge Yang:** Writing – review & editing. **Jiaxiang Chen:** Writing – review & editing. **David Wei Zhang:** Resources, Methodology. **Yuangang Wang:** Resources, Methodology. **Yuanjie Lv:** Resources, Methodology. **Zhihong Feng:** Resources, Methodology. **Xinbo Zou:** Writing – review & editing, Supervision, Resources, Funding acquisition, Conceptualization.

Declaration of competing interest

The authors declare that they have no known competing financial interests or personal relationships that could have appeared to influence the work reported in this paper.

Acknowledgment

This work was supported by ShanghaiTech University Startup Fund 2017F0203-000-14, the National Natural Science Foundation of China (Grant No. 52131303), and the Natural Science Foundation of Shanghai (Grant No. 22ZR1442300).

Data availability

Data will be made available on request.

References

[1] S. Pearton, F. Ren, M. Tadjer, J. Kim, Perspective: Ga_2O_3 for ultra-high power rectifiers and MOSFETS, J. Appl. Phys. 124 (2018) 220901, https://doi.org/10.1063/1.5062841.

[2] K.D. Chabak, K.D. Leedy, A.J. Green, S. Mou, A.T. Neal, T. Asel, E.R. Heller, N. S. Hendricks, K. Liddy, A. Crespo, N.C. Miller, M.T. Lindquist, N.A. Moser, R. C. Fitch, D.E. Walker, D.L. Dorsey, G.H. Jessen, Lateral β-Ga_2O_3 field effect transistors, Semicond. Sci. Technol. 35 (2019) 013002, https://doi.org/10.1088/1361-6641/ab55fe.

[3] Z. Wang, X. Chen, F.-F. Ren, S. Gu, J. Ye, Deep-level defects in gallium oxide, J. Phys. D Appl. Phys. 54 (2021) 043002, https://doi.org/10.1088/1361-6463/abbeb1.

[4] Y. Ma, X. Zhou, W. Tang, X. Zhang, G. Xu, L. Zhang, T. Chen, S. Dai, C. Bian, B. Li, Z. Zeng, S. Long, 702.3 A·cm^{-}2/10.4 mΩ·cm2 β-Ga_2O_3 U-shape trench gate MOSFET with N-ion implantation, IEEE Electron. Device Lett. 44 (2023) 384–387, https://doi.org/10.1109/LED.2023.3235777.

[5] A.Y. Polyakov, V.I. Nikolaev, E.B. Yakimov, F. Ren, S.J. Pearton, J. Kim, Deep level defect states in β-, α-, and ε-Ga_2O_3 crystals and films: impact on device performance, J. Vac. Sci. Technol. A 40 (2022) 020804, https://doi.org/10.1116/6.0001701.

[6] X. Xia, J.-S. Li, R. Sharma, F. Ren, M.A.J. Rasel, S. Stepanoff, N. Al-Mamun, A. Haque, D.E. Wolfe, S. Modak, L. Chernyak, M.E. Law, A. Khachatrian, S. J. Pearton, Radiation damage in the ultra-wide bandgap semiconductor Ga_2O_3, ECS J. Solid State Sci. Technol. 11 (2022) 095001, https://doi.org/10.1149/2162-8777/ac8bf7.

[7] A.Y. Polyakov, V.I. Nikolaev, A.I. Pechnikov, P.B. Lagov, I.V. Shchemerov, A. A. Vasilev, A.V. Chernykh, A.I. Kochkova, L. Guzilova, Y.S. Pavlov, T.V. Kulevoy, A.S. Doroshkevich, R.S. Isaev, A.V. Panichkin, S.J. Pearton, Carrier removal rates in 1.1 MeV proton irradiated α-Ga_2O_3 (Sn), J. Phys. D Appl. Phys. 56 (2023) 305103, https://doi.org/10.1088/1361-6463/acd06b.

[8] J. Kim, S.J. Pearton, C. Fares, J. Yang, F. Ren, S. Kim, A.Y. Polyakov, Radiation damage effects in Ga_2O_3 materials and devices, J. Mater. Chem. C (2019) 10–24, https://doi.org/10.1039/C8TC04193H, 10.1039/C8TC04193H 7.

[9] A. Petkov, D. Cherns, W.-Y. Chen, J. Liu, J. Blevins, V. Gambin, M. Li, D. Liu, M. Kuball, Structural stability of β-Ga_2O_3 under ion irradiation, Appl. Phys. Lett. 121 (2022) 171903, https://doi.org/10.1063/5.0120089.

[10] E. Farzana, A. Mauze, J.B. Varley, T.E. Blue, J.S. Speck, A.R. Arehart, S.A. Ringel, Influence of neutron irradiation on deep levels in Ge-doped (010) β-Ga_2O_3 layers grown by plasma-assisted molecular beam epitaxy, Apl. Mater. 7 (2019) 121102, https://doi.org/10.1063/1.5126463.

[11] E.B. Yakimov, A.Y. Polyakov, I.V. Shchemerov, N.B. Smirnov, A.A. Vasilev, P. S. Vergeles, E.E. Yakimov, A.V. Chernykh, A.S. Shikoh, F. Ren, S.J. Pearton, Photosensitivity of Ga_2O_3 Schottky diodes: effects of deep acceptor traps present before and after neutron irradiation, Apl. Mater. 8 (2020) 111105, https://doi.org/10.1063/5.0030105.

[12] A.Y. Polyakov, N.B. Smirnov, I.V. Shchemerov, A.A. Vasilev, E.B. Yakimov, A. V. Chernykh, A.I. Kochkova, P.B. Lagov, Y.S. Pavlov, O.F. Kukharchuk, A. A. Suvorov, N.S. Garanin, I.-H. Lee, M. Xian, F. Ren, S.J. Pearton, Pulsed fast reactor neutron irradiation effects in Si doped n-type β-Ga_2O_3, J. Phys. D Appl. Phys. 53 (2020) 274001, https://doi.org/10.1088/1361-6463/ab83c4.

[13] H. Gao, S. Muralidharan, M.R. Karim, L.R. Cao, K.D. Leedy, H. Zhao, S. Rajan, D. C. Look, L.J. Brillson, Depth-resolved cathodoluminescence and surface photovoltage spectroscopies of gallium vacancies in β-Ga_2O_3 with neutron irradiation and forming gas anneals, J. Vac. Sci. Technol. B 39 (2021) 052205, https://doi.org/10.1116/6.0001240.

[14] H. Gao, S. Muralidharan, N. Pronin, M.R. Karim, S.M. White, T. Asel, G. Foster, S. Krishnamoorthy, S. Rajan, L.R. Cao, M. Higashiwaki, H. von Wenckstern, M. Grundmann, H. Zhao, D.C. Look, L.J. Brillson, Optical signatures of deep level defects in Ga_2O_3, Appl. Phys. Lett. 112 (2018) 242102, https://doi.org/10.1063/1.5026770.

[15] M.E. Ingebrigtsen, A.Y. Kuznetsov, B.G. Svensson, G. Alfieri, A. Mihaila, U. Badstübner, A. Perron, L. Vines, J.B. Varley, Impact of proton irradiation on conductivity and deep level defects in β-Ga_2O_3, Apl. Mater. 7 (2018) 022510, https://doi.org/10.1063/1.5054826.

[16] A.Y. Polyakov, N.B. Smirnov, I.V. Shchemerov, E.B. Yakimov, J. Yang, F. Ren, G. Yang, J. Kim, A. Kuramata, S.J. Pearton, Point defect induced degradation of electrical properties of Ga_2O_3 by 10 MeV proton damage, Appl. Phys. Lett. 112 (2018) 032107, https://doi.org/10.1063/1.5012993.

[17] A.Y. Polyakov, N.B. Smirnov, I.V. Shchemerov, E.B. Yakimov, S.J. Pearton, C. Fares, J. Yang, F. Ren, J. Kim, P.B. Lagov, V.S. Stolbunov, A. Kochkova, Defects responsible for charge carrier removal and correlation with deep level introduction in irradiated β-Ga_2O_3, Appl. Phys. Lett. 113 (2018) 092102, https://doi.org/10.1063/1.5049130.

[18] M.E. Ingebrigtsen, J.B. Varley, A.Y. Kuznetsov, B.G. Svensson, G. Alfieri, A. Mihaila, U. Badstübner, L. Vines, Iron and intrinsic deep level states in Ga_2O_3, Appl. Phys. Lett. 112 (2018) 042104, https://doi.org/10.1063/1.5020134.

[19] J. Lee, E. Flitsiyan, L. Chernyak, J. Yang, F. Ren, S.J. Pearton, B. Meyler, Y. J. Salzman, Effect of 1.5 MeV electron irradiation on β-Ga_2O_3 carrier lifetime and diffusion length, Appl. Phys. Lett. 112 (2018) 082104, https://doi.org/10.1063/1.5011971.

[20] Z. Zhang, T. Wang, L. Xiao, C. Liu, J. Zhou, Y. Zhang, C. Qi, G. Ma, M. Huo, Effect of electron irradiation and defect analysis of β-Ga_2O_3 Schottky barrier diodes, IEEE Trans. Electron. Dev. 71 (2024) 1676–1680, https://doi.org/10.1109/TED.2023.3334713.

[21] N. Manikanthababu, H. Sheoran, K. Prajna, S.A. Khan, K. Asokan, J.V. Vas, R. Medwal, B.K. Panigrahi, R. Singh, Electrical characteristics and defect dynamics induced by swift heavy ion irradiation in Pt/PtO/β-Ga_2O_3 vertical Schottky barrier diodes, IEEE Trans. Electron. Dev. 69 (2022) 5996–6001, https://doi.org/10.1109/TED.2022.3207702.

[22] W.-S. Ai, J. Liu, Q. Feng, P.-F. Zhai, P.-P. Hu, J. Zeng, S.-X. Zhang, Z.-Z. Li, L. Liu, X.-Y. Yan, Y.-M. Sun, Degradation of β-Ga_2O_3 Schottky barrier diode under swift heavy ion irradiation, Chin. Phys. B 30 (2021) 056110, https://doi.org/10.1088/1674-1056/abf107.

[23] J.F. McGlone, H. Ghadi, E. Cornuelle, A. Armstrong, G. Burns, Z. Feng, A.F.M. A. Uddin Bhuiyan, H. Zhao, A.R. Arehart, S.A. Ringel, Proton radiation effects on electronic defect states in MOCVD-grown (010) β-Ga_2O_3, J. Appl. Phys. 133 (2023) 045702, https://doi.org/10.1063/5.0121416.

[24] R. Sun, A.R. Balog, H. Yang, N. Alem, M.A. Scarpulla, Degradation of β-Ga_2O_3 vertical Ni/Au Schottky diodes under forward bias, IEEE Electron. Device Lett. 44 (2023) 725–728, https://doi.org/10.1109/LED.2023.3258644.

[25] Y. Zhang, J. Zhang, Z. Feng, Z. Hu, J. Chen, K. Dang, Q. Yan, P. Dong, H. Zhou, Y. Hao, Impact of implanted edge termination on vertical β-Ga_2O_3 Schottky barrier diodes under OFF-state stressing, IEEE Trans. Electron. Dev. 67 (2020) 3948–3953, https://doi.org/10.1109/TED.2020.3002327.

[26] H. Qu, W. Huang, Y. Zhang, J. Sui, J. Chen, B. Chen, D.W. Zhang, Y. Wang, Y. Lv, Z. Feng, X. Zou, Reliable electrical performance of β-Ga_2O_3 Schottky barrier diode at cryogenic temperatures, J. Vac. Sci. Technol. A 42 (2024) 023418, https://doi.org/10.1116/6.0003298.

[27] E.R. Benton, E.V. Benton, Space radiation dosimetry in low-Earth orbit and beyond, Nucl. Instrum. Methods Phys. Res., Sect. B 184 (2001) 255–294, https://doi.org/10.1016/S0168-583X(01)00748-0.

[28] M. Higashiwaki, K. Konishi, K. Sasaki, K. Goto, K. Nomura, Q. Thieu, R. Togashi, H. Murakami, Y. Kumagai, B. Monemar, A. Koukitu, A. Kuramata, S. Yamakoshi, Temperature-dependent capacitance–voltage and current–voltage characteristics of Pt/Ga_2O_3 (001) Schottky barrier diodes fabricated on n^{-}–Ga_2O_3 drift layers grown by halide vapor phase epitaxy, Appl. Phys. Lett. 108 (2016) 133503, https://doi.org/10.1063/1.4945267.

[29] Z. Wang, H. Gong, C. Meng, X. Yu, X. Sun, C. Zhang, X. Ji, F. Ren, S. Gu, Y. Zheng, R. Zhang, J. Ye, Majority and minority carrier traps in NiO/β-Ga2O3 p^{+}-n heterojunction diode, IEEE Trans. Electron. Dev. 69 (2022) 981–987, https://doi.org/10.1109/TED.2022.3143491.

[30] S.J. Pearton, F. Ren, E. Patrick, M.E. Law, A.Y. Polyakov, Review—ionizing radiation damage effects on GaN devices, ECS J. Solid State Sci. Technol. 5 (2016) Q35, https://doi.org/10.1149/2.0251602jss.

[31] J.-S. Li, C.-C. Chiang, X. Xia, H.-H. Wan, J. Kim, F. Ren, S.J. Pearton, 15 MeV proton damage in NiO/β-Ga_2O_3 vertical rectifiers, J. Phys.: Mater. 6 (2023) 045003, https://doi.org/10.1088/2515-7639/acef98.

[32] D. Wang, R. Hu, G. Chen, C. Tang, Y. Ma, M. Gong, Q. Yu, S. Cao, Y. Li, M. Huang, Z. Yang, Heavy ion radiation and temperature effects on SiC Schottky barrier diode, Nucl. Instrum. Methods Phys. Res., Sect. B 491 (2021) 52–58, https://doi.org/10.1016/j.nimb.2021.01.019.

[33] P.K. Rao, B. Park, S.-T. Lee, Y.-K. Noh, M.-D. Kim, J.-E. Oh, Analysis of leakage current mechanisms in Pt/Au Schottky contact on Ga-polarity GaN by Frenkel-Poole emission and deep level studies, J. Appl. Phys. 110 (2011) 013716, https://doi.org/10.1063/1.3607245.

[34] K.R. Peta, B.-G. Park, S.-T. Lee, M.-D. Kim, J.-E. Oh, T.-G. Kim, V.R. Reddy, Analysis of electrical properties and deep level defects in undoped GaN Schottky barrier diode, Thin Solid Films 534 (2013) 603–608, https://doi.org/10.1016/j.tsf.2013.01.100.

[35] A. Jayawardena, A.C. Ahyi, S. Dhar, Analysis of temperature dependent forward characteristics of Ni/($\bar{2}$01) β-Ga_2O_3 Schottky diodes, Semicond. Sci. Technol. 31 (2016) 115002, https://doi.org/10.1088/0268-1242/31/11/115002.

[36] L. Zhou, X. Lu, L. Chen, X. Ouyang, B. Liu, J. Xu, H. Tang, Leakage current by poole–frenkel emission in Pt Schottky contacts on ($\bar{2}$01) β-Ga_2O_3 grown by edge-defined film-fed growth, ECS J. Solid State Sci. Technol. 8 (2019) Q3054, https://doi.org/10.1149/2.0111907jss.

[37] Y. Zhang, X. Zhang, M. Zhu, J. Chen, C.W. Tang, K.M. Lau, X. Zou, Forward conduction instability of quasi-vertical GaN p-i-n diodes on Si substrates, IEEE Trans. Electron. Dev. 67 (2020) 3992–3998, https://doi.org/10.1109/TED.2020.3012422.

[38] K. Kanegae, M. Horita, T. Kimoto, J. Suda, Accurate method for estimating hole trap concentration in n-type GaN via minority carrier transient spectroscopy, Appl. Phys. Express 11 (2018) 071002, https://doi.org/10.7567/apex.11.071002.

[39] A.Y. Polyakov, N.B. Smirnov, I.V. Shchemerov, D. Gogova, S.A. Tarelkin, S. J. Pearton, Compensation and persistent photocapacitance in homoepitaxial Sn-doped β-Ga_2O_3, J. Appl. Phys. 123 (2018) 115702, https://doi.org/10.1063/1.5025916.

[40] A. Coelho, M. Adam, H. Boudinov, Distinguishing bulk traps and interface states in deep-level transient spectroscopy, J. Phys. D Appl. Phys. 44 (2011) 305303, https://doi.org/10.1088/0022-3727/44/30/305303.